

## Refinement of the Crystal Structure of Taurine, 2-Aminoethylsulfonic Acid An Example of Computer-Controlled Experimentation

BY Y. OKAYA

*IBM Watson Research Center, Yorktown Heights, New York, U.S.A.*

(Received 18 February 1966)

The crystal structure of taurine, 2-aminoethylsulfonic acid, was refined from three-dimensional intensity data collected on a computer-controlled diffractometer operated by an IBM 1620 machine under a stored data-collection program. The crystal belongs to the monoclinic system with  $a = 5.27_9$ ,  $b = 11.64_5$ ,  $c = 7.93_1$  Å,  $\beta = 94.1^\circ$ ; the space group is  $P2_1/c$ . The positions of all the hydrogen atoms were obtained by a three-dimensional ( $F_o - F_c$ ) synthesis.

The molecule possesses the zwitterion configuration with the formula  $\text{NH}_3^+ - \text{CH}_2 - \text{CH}_2 - \text{SO}_3^-$ ; the amino and sulfonate groups assume a *gauche* configuration around the central methylene linkage. All bond distances and angles in the zwitterion are of normal values.

The molecules are held in the structure by a three-dimensional network of N-H...O hydrogen bonds of the usual strength. A brief discussion on the program for computer-controlled data collection is also presented.

### Introduction

This work is part of the project currently undertaken by the author on systematic studies on the precise molecular configurations of aliphatic amino acids with acidic groups other than carboxyl groups. Taurine, 2-aminoethylsulfonic acid, is commonly found in animals, and the knowledge of its configuration is important in understanding the metabolism of some amino acids in such a physiological environment. The crystal structure of taurine has been studied by Sutherland & Young (1963) based on three-dimensional diffraction data obtained by the photographic method. Although there is little doubt about the heavy-atom positions deduced from such data, it is difficult to accept some of the conclusions given by the authors based on the hydrogen atom positions obtained by a difference electron-density synthesis; this is especially so in view of the presence of rather heavy sulfur atoms in the structure and a relatively high  $R$  index (11% for observed reflections only). Since these authors, on the basis of their data, have not located three hydrogen atoms around the amino nitrogen atom, they have concluded that taurine might not be a zwitterion. In view of the bond distances and angles found in the taurine molecule it is quite difficult to accept the non-zwitterion structure; moreover it has been established by X-ray and neutron diffraction methods that many other similar amino acids with varieties of acidic groups possess zwitterion configurations.

Since the knowledge of the correct nature of taurine is important in understanding the biological role of the molecule, it seemed worthwhile to reinvestigate its crystal structure by more accurate and comprehensive intensity data. The present paper deals with three-

dimensional refinement of the structure using intensity data collected on our computer-controlled diffractometer (Cole, Okaya & Chambers, 1963). The work might also be used as an example of continuous flow of computer usage in crystallography. After the definition of the problem and manipulation of specimens, the computers play crucial roles in all the subsequent phases of the crystallographic study; they include data collection, data analyses, and finally presentation of the results.

A needle-shaped single crystal of taurine was cut and ground into an approximately spherical shape of about 0.3 mm in diameter and mounted on a General Electric goniostat which was placed on a Picker biplane diffractometer. The diffractometer is part of the CCXD, a computer-controlled diffractometer system which is operated in a closed-loop manner by an IBM 1620 machine under a stored data collection program. As the first step of automatic\* data collection processes, the cell constants were studied by using Mo  $K\alpha$  radiation on the diffractometer. The cell dimensions thus obtained are:  $a = 5.27_9$ ,  $b = 11.64_5$ ,  $c = 7.93_1$  Å,  $\beta = 94.1^\circ$ ;  $a:b:c = 0.4533:1:0.6811$ . These axial ratios are in relatively good agreement with those listed by Groth (1910) (0.4539:1:0.6827 by exchanging  $a$  and  $c$ ). The observed cell constants were so chosen that the  $2\theta$  values of reflections can be calculated within the tolerance of the diffractometer system in the range of  $2\theta$  employed in the present study. The space group  $P2_1/c$  as given by Sutherland & Young is employed without further checking the systematic absences.

\* We should draw a clear distinction between a simply automated system and a computer-controlled system; however, the adjective *automatic* is used here in such a way as to describe processes which require minimum participation of human beings in repetitive operations including combinations of hardware manipulations as well as logical decisions.

\* Work supported in part by AFCRL 19(628)-2469.

### Computer-controlled data collection

Three-dimensional integrated intensity data within the range of  $\sin \theta/\lambda \leq 0.91$  were obtained from the specimen by again using Mo  $K\alpha$  radiation. Since the computer-controlled diffractometer system has been used successfully in the past two years on the structure analyses of more than two dozen crystals, it might be justifiable to explain briefly the actual computer program used in the data collection.

The program is divided into two parts. The first part deals with the initialization of the task; from the cell constants and orientation of the crystal are calculated the corresponding values for the reciprocal lattice. If requested, the upper limits of the Miller indices are established for the range of  $\sin \theta/\lambda$  given as an input parameter and other necessary housekeeping work. After this initialization has been performed, this part of the program can be overlaid by the main data collection program.

The second part concerns the actual data collection which can be divided into two sub-parts, one which is relatively independent of the crystals being examined or the methods of data collection and the other part, a subroutine for manipulating the diffractometer, which might have to be modified according to the mode of data collection. The former generates all possible points in reciprocal space within the specified  $\sin \theta/\lambda$  range in the order given by input data. In order to shorten the time required in moving through reciprocal space, the reflections were generated as shown in Fig. 1. This method of generating the reciprocal lattice points may not make the traveling time minimum; however as discussed later, the data collection scheme employed presently spends more time around each reciprocal lattice point than that required for traveling from one point to the next, and this method of generating reciprocal lattice points does not seem too unreasonable. The reciprocal lattice points must of course be tested for the systematic absences or any

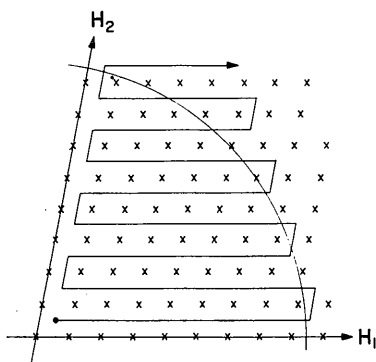


Fig. 1. The method of generating reflections used by the present program in a constant  $H_3$  section.  $H_1$  is the most frequently changing index, usually along the longest real cell dimension (or the shortest for reciprocal lattice).  $H_3$  (not shown in the figure) is the least frequently changing Miller index. The negative sides of  $H_1$  and/or  $H_2$  can also be generated in the same manner.

other conditions imposed by the experimental need. These restrictions can be expressed by rewriting this portion of the subroutine for each problem.

The subroutine used in manipulating the diffractometer may have to be modified but not necessarily be rewritten for each crystal. The basic concept in programming for such a hardware control operation is to ensure steady flow of manipulation with maximum possible care in checking the validity of obtained data. It should be emphasized here that by having a computer-controlled diffractometer system, it is not possible to speed up the data collection task into the millisecond realm. The advantage is gained only by continuous, steady operation, elimination of clerical mistakes and use of logical ability of computers to test the obtained results at the time they are obtained.

From the programming standpoint, the diffractometer can be treated as an  $I/O$  (input-output) unit, from and to which information exchange can be made by the computer. The output from the computer is considered as commands to the diffractometer; they include new angular settings, presetting values of the counting devices, new attenuator settings and others. Input to the computer is usually the experimental conditions of the diffractometer such as present angular settings, contents of the counting devices, the filter settings and the status of the hardware. The computer also performs the following control tasks: to start and stop motors, preset, reset and start the counting devices, place the filters and attenuators in the X-ray beam, and others. For actual detailed discussion of the diffractometer system, refer to our previous article (Cole, Okaya & Chambers, 1963). In order to achieve the most important merit of computer control, it becomes necessary to program the subroutine in such a way that the experiments can be performed with the same kind of attention as given by a human operator; it is rather remarkable that, during the performance of an experiment, many logical decisions are actually made by the human operator, either consciously or subconsciously. In Fig. 2, a flow diagram of the logical decisions made by the computer after each measurement (count, in the case of diffraction experiments) is demonstrated.

The three-dimensional data used in the present analysis of the structure of taurine were obtained under the principle outlined above by using filtered Mo  $K\alpha$  radiation. For each reflection, the alignment of the crystal and the instrument were first studied by optimizing the  $\omega$  setting on the biplane diffractometer\*. The integrated intensity was then recorded by step-scanning around the  $2\theta$  axis; the number of steps used is 24. The intervals of the  $2\theta$  step scanning had been

\* If intensity measurements are made at large  $2\theta$  values (usually when a longer wavelength is employed), it might also become necessary to study the  $\chi$  setting. For certain experimental conditions, the effect of missetting the  $\chi$  arc becomes more important than that of the  $\omega$  direction for reflections with large  $2\theta$  values.

determined by checking the profile of several reflections in various  $2\theta$  ranges; they were  $9/100^\circ$  for reflections below  $40^\circ$  in  $2\theta$  and  $11/100^\circ$  thereabove. These intervals were determined in such a way that the first three and the last three steps out of the 24  $2\theta$  step-scan data for a reflection do represent the background at its  $2\theta$  value. These values are also dependent on the experimental conditions – such as the speed of data collection, use of a monochromator, and others. In the course of optimizing the  $\omega$  setting of a reflection, the maximum and minimum counts were recorded and if the difference between them was less than the statistical fluctuation, the reflection was treated as a non-observed one. The detailed data collection program, written in the IBM 1620 SPS (Symbolic Programming System) language, is explained elsewhere (Okaya, 1964). In order to facilitate the programming tasks, the programming system had also been modified to accommodate additional instruction sets required for the hardware manipulation. Out of the 3124 non-equivalent reflections accessible within the region of  $\sin \theta/\lambda \leq 0.91$ , 2639 reflections were recorded as observed. This relatively large number of non-observed reflections is due to the  $2\theta$  limit value, which is high for reflections from such an organic compound, and also the rather stringent condition in accepting the intensity data.

The integrated intensity data of reflections were calculated from the data on count, time, and attenuator settings for the 24 steps on the  $(\theta-2\theta)$  step scanning. The computation was done as a time-shared program on the 1620. On account of the small linear absorption

coefficient of the sample for the Mo radiation, no absorption correction was made.

### Refinement of the structure

The structure was refined in a straightforward fashion by using the three-dimensional data thus obtained. Starting from the values given by Sutherland & Young (1963), the atomic coordinates of the seven non-hydrogen atoms were refined by using a full-matrix least-squares program on an IBM 7094 computer (Okaya, 1963); the isotropic temperature factors given by them were converted into the corresponding anisotropic temperature factors and also used as the starting parameters. The positions of hydrogen atoms were then studied by the usual three-dimensional ( $F_o - F_c$ ) synthesis method. All the four hydrogen atoms on the two carbon atoms were located at positions close to those given by Sutherland & Young (1963). However, contrary to their results, three peaks were located around the nitrogen; these three peaks are at distances of about  $0.9 \text{ \AA}$  from the nitrogen and, together with the carbon atom bonded to it, form a tetrahedral arrangement around the nitrogen. Two of these peaks are near the positions of the two hydrogen atoms, H(5) and H(6), given in the previous article; no electron density was found around its last hydrogen atom, H(7). A composite diagram of the difference synthesis is shown in Fig. 3. The atomic coordinates of these seven hydrogen atoms were then subjected to the least-squares treatment by assigning isotropic temperature

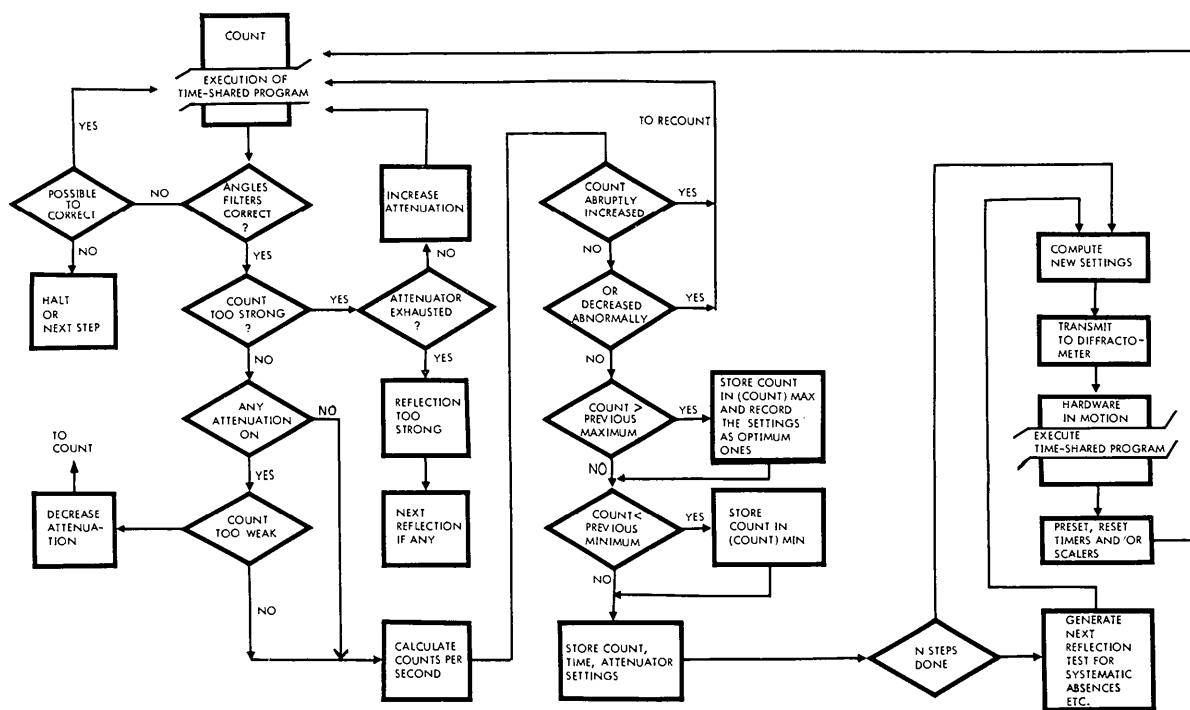


Fig. 2. A flow chart of the data collection scheme stressing logical decisions made by the computer to ensure the validity of the obtained data. After each measurement (or count), the computer tests for any abnormal condition which invalidates the results. This decision-making routine is, as programming technique, a copy of decisions made by a *conscientious* human operator.

factors to account for their thermal motions. The final conventional error factor  $R = \sum ||F_o| - |F_c|| / \sum |F_o|$  was reduced to 0.040 for the observed reflections (or 0.059 when all accidentally absent reflections were introduced

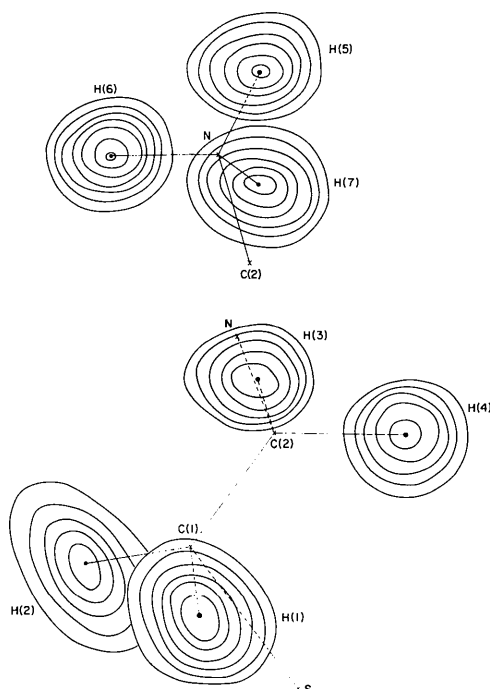


Fig. 3. A composite diagram of the electron-density function associated with the hydrogen atoms; the contours are drawn at equal intervals of 0.1 e.Å<sup>-3</sup> starting from 0.2 e.Å<sup>-3</sup>.

Table 1(a). Atomic coordinates in fractions of cell edges and their standard deviations,  $\sigma$  (in 10<sup>-4</sup> Å)

The standard deviations of the hydrogen atoms are 0.02–0.03 Å.

	$x$	$\sigma(x)$	$y$	$\sigma(y)$	$z$	$\sigma(z)$
S	0.29666	2	0.15131	2	0.14910	3
O(1)	0.56437	8	0.16291	9	0.20700	13
O(2)	0.15802	10	0.25869	10	0.14570	12
O(3)	0.26797	9	0.08903	10	-0.01156	9
C(1)	0.16033	11	0.06153	11	0.30006	12
C(2)	0.28932	11	-0.05490	12	0.31863	12
N	0.23581	9	-0.12925	10	0.16840	10
H(1)	0.175		0.105		0.403	
H(2)	-0.015		0.056		0.260	
H(3)	0.234		-0.090		0.417	
H(4)	0.466		-0.044		0.342	
H(5)	0.290		-0.200		0.191	
H(6)	0.086		-0.129		0.139	
H(7)	0.305		-0.094		0.090	

Table 1(b). Anisotropic temperature factors

$\beta$ 's are used in the usual formula  $\exp \{-(\beta_{11}h^2 + \beta_{22}k^2 + \beta_{33}l^2 + \beta_{12}hk + \beta_{13}hl + \beta_{23}kl)\}$ .

	$\beta_{11}$	$\beta_{22}$	$\beta_{33}$	$\beta_{12}$	$\beta_{13}$	$\beta_{23}$
S	0.01275	0.00230	0.00899	0.00080	0.00324	-0.00036
O(1)	0.01450	0.00406	0.01814	-0.00375	-0.00227	-0.00212
O(2)	0.02862	0.00334	0.01503	0.00878	0.01138	0.00190
O(3)	0.02184	0.00424	0.00832	0.00017	0.00503	-0.00090
C(1)	0.01793	0.00350	0.00807	0.00015	0.00537	-0.00061
C(2)	0.02011	0.00354	0.00850	-0.00056	-0.00235	-0.00163
N	0.01720	0.00293	0.00924	0.00083	0.00396	0.00049

Table 1(c). Isotropic temperature factors for hydrogen atoms (in 10<sup>-16</sup> cm<sup>2</sup>)

H(1)	H(2)	H(3)	H(4)	H(5)	H(6)	H(7)
1.2	1.6	0.9	2.1	1.1	0.6	2.1

as  $F_o \equiv 0$ ). The atomic coordinates, their standard deviations and thermal parameters at the final stage are listed in Table 1. The shifts of parameters at this stage are quite negligible. To confirm further our basis for rejecting the previous H(7) position, the similar calculation was performed by replacing the coordinates of H(7) in Table 1 by the values for H(7) in the previous report. This gave an  $R$  of 0.044 (for the observed reflections only) with subsequent abnormal increase in the temperature factor of this hydrogen atom\*. Except for this seventh hydrogen atom, the coordinates given in the previous paper are correct within reasonable multiples of their standard deviations. The following are some of the computational details for the data-analysis stage. All the necessary computation was done on an IBM 7094 machine at the IBM Research Center; the atomic scattering factors used in the structure factor calculations were obtained from the values in *International Tables for X-ray Crystallography*. The weighting scheme used in the least-squares analysis is  $\omega = 1.0$  for  $|F_{obs}| \leq 20.0$  and  $\omega = 20.0/|F_{obs}|$  for  $|F_{obs}| \geq 20.0$  and unobserved reflections were given zero weight; this weighting scheme is employed to represent errors in observed structure factors rather realistically, and not those in observed intensities. Comparison between the observed and calculated structure factors is given in Table 2. Interatomic distances and bond angles were calculated from the atomic coordinates in Table 1(a).

### Discussion of the results

The present study on the crystal structure of taurine has established unambiguously that taurine possesses the zwitterion configuration and its structural formula is written as  $\text{NH}_3^+ - \text{CH}_2 - \text{CH}_2 - \text{SO}_3^-$ . As shown in Fig. 4, the zwitterion possesses a *gauche* configuration around the central methylene linkage. Fig. 5 shows bond distances in the taurine molecule, and in Table 3 are listed bond angles.

The configuration of the sulfonate group is rather interesting. O(1) and O(3), which are involved in rela-

\* There is hardly any need to consult the table of Hamilton (1965) in deciding which of the two positions is the correct one for the seventh hydrogen atom.

Table 2. Comparison between the observed and calculated structure factors

The values in the Table have been multiplied by 10

Table with columns for FO, FC, and HxK values. The table contains multiple columns of data representing observed and calculated structure factors for various HxK indices. The values are integers, some with leading zeros, and are arranged in a grid-like format.

Table 2 (cont.)

A large table with multiple columns and rows of numerical data, organized in a grid-like structure with various sub-headers.



tively strong N-H---O hydrogen bonds, have equivalent S-O distances, whereas O(2), which is only loosely associated with an amino group, exhibits a smaller separation of 1.448 Å. The C(1)-S distance of 1.780 Å is a normal one for such an aliphatic molecule.

The average O-S-O and C-S-O angles in the sulfonate group are 112.9 and 106.7°, respectively. These deviations from the tetrahedral angle of 109.5° are commonly found in aliphatic as well as aromatic sulfonates and also in other ions with -X-SO<sub>3</sub><sup>-</sup> groups, X replacing the C. Other bond distances and angles in the molecule are quite normal; as is usual, the

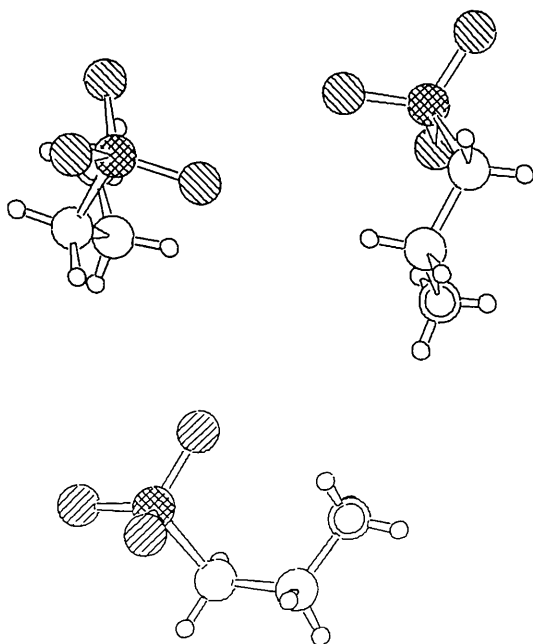


Fig. 4. Several views of the taurine molecule showing the conformation around the central methylene linkage. Open circles, carbon; double circles, nitrogen; shaded circles, oxygen; double-shaded circles, sulfur.

average C-H and N-H distances of 0.95 and 0.85 Å, respectively, are much shorter than those found by the neutron diffraction method.

In the crystal structure, the molecules are held together by a three-dimensional network of N-H---O

Table 3. *Taurine*: bond angles

Around S			
O(1)-S-O(2)	113.7°	O(1)-S-C(1)	105.8°
O(1)-S-O(3)	110.9	O(2)-S-C(1)	106.9
O(2)-S-O(3)	113.0	O(3)-S-C(1)	105.8
Around C(1)			
S-C(1)-C(2)	112.9	H(1)-C(1)-C(2)	112
S-C(1)-H(1)	105	H(2)-C(1)-C(2)	113
S-C(1)-H(2)	104	H(1)-C(1)-H(2)	109
Around C(2)			
C(1)-C(2)-N	112.6	H(3)-C(2)-N	111
C(1)-C(2)-H(3)	107	H(4)-C(2)-N	111
C(1)-C(2)-H(4)	109	H(3)-C(2)-H(4)	105
Around N			
C(2)-N-H(5)	111	H(5)-N-H(6)	110
C(2)-N-H(6)	111	H(5)-N-H(7)	117
C(2)-N-H(7)	104	H(6)-N-H(7)	104

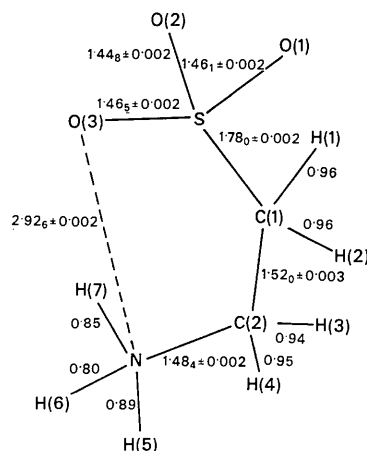


Fig. 5. Bond distances in the taurine molecule. The intramolecular N-O separation is shown by a dotted line.

Table 4

(a) Short N-O contacts.

No.	Atom	Equivalent position	Distance	Hydrogen atom involved	N-H-O angle	O-H separations
I	O(1)	(1-x, -½+y, ½-z)	2.79 <sub>3</sub> Å	H(5)	166°	1.9 <sub>2</sub>
II	O(3)	(-x, -y, -z)	2.89 <sub>3</sub>	H(6)	162	2.1 <sub>2</sub>
III	O(2)	(-x, -½+y, ½-z)	2.93 <sub>9</sub>	H(6)	110	2.5 <sub>6</sub>
IV	O(3)	(1-x, -y, -z)	3.01 <sub>6</sub>	H(7)	132	2.3 <sub>8</sub>
V	O(3)	intramolecular	2.92 <sub>6</sub>	H(7)	133	2.2 <sub>9</sub>

(b) Configuration around N  
Angles between and

C-N	I	100.1°
C-N	II	111.5
C-N	IV	96.8
C-N	V	82.5
I	II	127.2
I	IV	87.9
I	V	153.1
II	IV	127.6
II	V	74.5



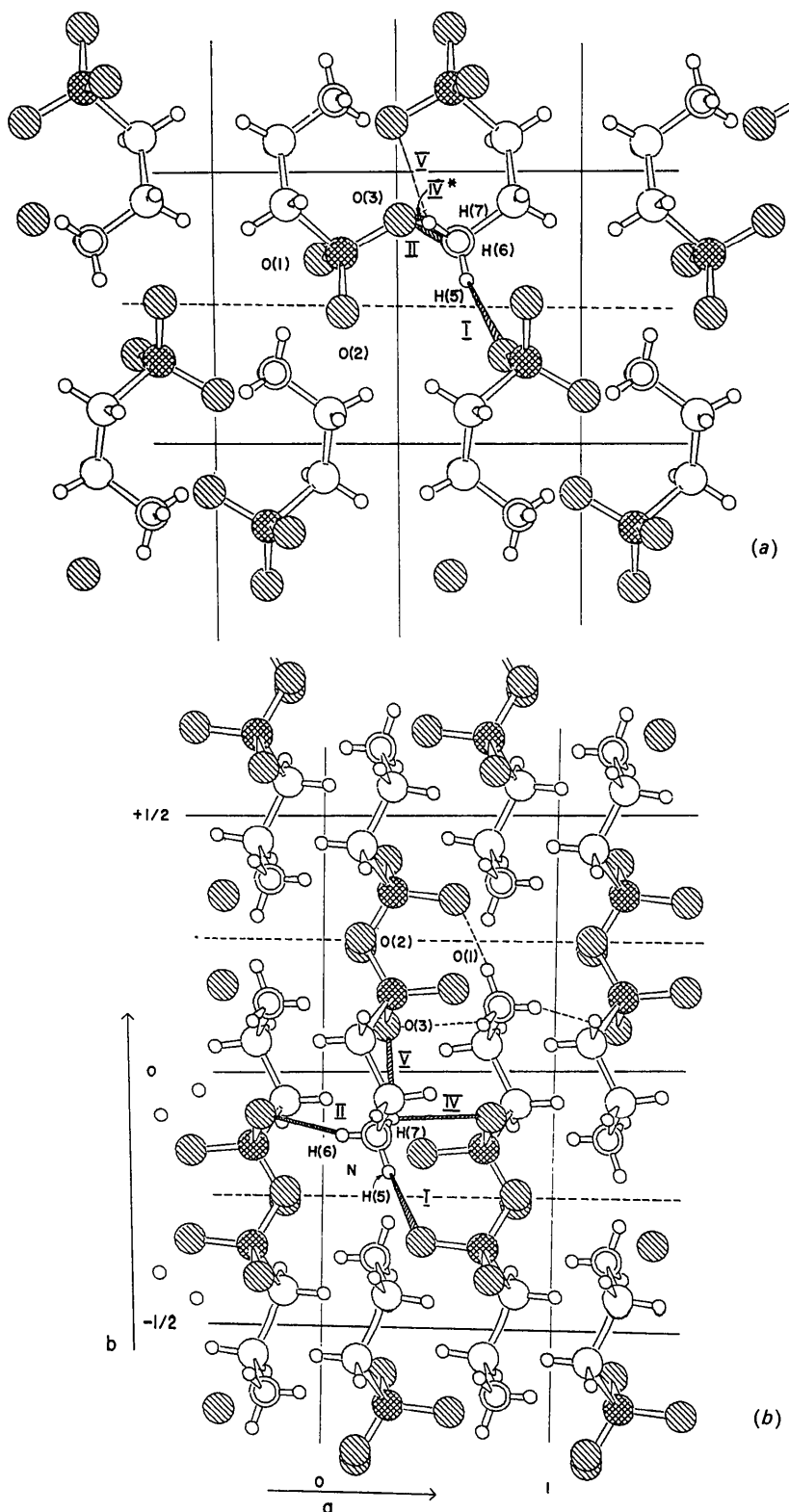


Fig. 6. (a) View of the structure projected down the  $a$  axis. The N-O contacts discussed in the text (and Table 4) are shaded. H(6) is almost under the nitrogen atom. Bond IV\* goes to O(3), which is one unit cell above along the  $a$  axis. (b) Projection of the structure along the  $c$  axis. These two drawings and Fig. 4 were drawn on an IBM 1627 machine based on calculations done by a structure drawing program on an IBM 7094 (Okaya, 1966). Except for adding the necessary information for the hydrogen-bond system and unit-cell outlines, these drawings have not been retouched.

hydrogen bonds. The assignment of hydrogen bonds to observed short N–O contacts can be made with the help of the hydrogen positions. In Table 4(a), five N–O contacts which are within hydrogen bond distances are listed together with the angles around the hydrogen atoms. The contact III with a relatively sharp N–H–O angle can be eliminated as a hydrogen bond; therefore contacts I and II are considered as the hydrogen bonds formed by H(5) and H(6), respectively. For H(7), there are two choices, IV and V; although the configuration around the nitrogen atoms [Table 4 (b)] seems to favor contact IV as the hydrogen bond formed by H(7), the evidence is not strong enough to preclude the fifth (intramolecular) contact as a possible one. It is also possible to consider that H(7) is actually involved in a bifurcated hydrogen bond system with these two contacts. In either case, O(3) is involved in two hydrogen bonds; this is rather interesting because the S–O(1) and S–O(3) bond lengths are almost the same, although O(1) is involved in only one hydrogen bond. A similar situation was found in the structure of D-tartaric acid, where the two carboxyl groups in the molecule exhibit almost equal C=O distances, although one of these two double bonded oxygen atoms receives two hydrogen bonds whereas the other receives only one (Okaya,

Stemple & Kay, 1966). As discussed before, O(2) with a short S–O bond is not involved in hydrogen bond formation. Fig. 6 shows drawings of the structure viewed down the *a* and *c* axes. The hydrogen bond system is illustrated in the drawings by shaded lines.

The author is indebted to N.R. Stemple for his help in collecting intensity data on the CCXD.

#### References

- COLE, H., OKAYA, Y. & CHAMBERS, F. W. (1963). *Rev. Sci. Instrum.* **34**, 872.  
 GROTH, P. (1910). *Chemische Krystallographie*. Vol. III, p. 159. Leipzig: Engelmann.  
 HAMILTON, W. C. (1965). *Acta Cryst.* **18**, 502.  
 OKAYA, Y. (1963). A.C.A. Computing Conference, March 1963, IBM Research Center, Yorktown Heights, New York.  
 OKAYA, Y. (1964). Control Programs for CCXD; unpublished report.  
 OKAYA, Y. (1966). Paper presented at A.C.A. Annual Meeting, Austin, Texas, March 1966.  
 OKAYA, Y., STEMPLE, N. R. & KAY, M. I. (1966). *Acta Cryst.* **21**, 237.  
 SUTHERLAND, H. H. & YOUNG, D. W. (1963). *Acta Cryst.* **16**, 897.

*Acta Cryst.* (1966). **21**, 735

### The Structure of Decammine- $\mu$ -peroxo-dicobalt Monosulfate Tris(bisulfate)\*

BY WILLIAM P. SCHAEFER AND RICHARD E. MARSH

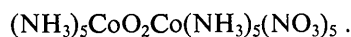
*Gates and Crellin Laboratories of Chemistry, California Institute of Technology, Pasadena, California 91109, U.S.A.*

(Received 23 February 1966)

Decammine- $\mu$ -peroxo-dicobalt monosulfate tris(bisulfate),  $(\text{NH}_3)_5\text{CoO}_2\text{Co}(\text{NH}_3)_5\text{SO}_4(\text{HSO}_4)_3$ , crystallizes in the orthorhombic space group  $P2_12_12_1$  with  $a=16.36$ ,  $b=13.95$ , and  $c=9.98$  Å; there are four formula units in the cell. The structure was determined by Patterson and trial-and-error methods and refined by three-dimensional least-squares calculations based on 1458 reflections. The final *R* index is 0.078 and the standard deviations in the coordinates are about 0.003, 0.005, 0.02, and 0.02 Å for the Co, S, N, and O atoms.

The coordinating ligands about the cobalt atoms form nearly regular octahedra with Co–N and Co–O distances of 1.95 and 1.89 Å. The Co–O–O–Co group is planar, with the bridging peroxide group skewed to the Co–Co axis; the O–O distance is 1.31 Å and the Co–O–O angles are 118°. The ions are held together by a very extensive network of hydrogen bonds which appears to involve all 33 hydrogen atoms.

Recently Vannerberg & Brosset (VB; 1963) have reported the results of a crystal-structure investigation of the bridged dicobalt compound decammine- $\mu$ -peroxo-dicobalt pentanitrate,



They reported the O–O axis of the bridging peroxide group to be perpendicular to the Co–Co axis, a configuration in agreement with that postulated earlier by Vlček (1960) for the decammine- $\mu$ -peroxo-dicobalt(5+) cation; this configuration could result, according to Vlček, from overlap of cobalt *d*-orbitals with  $\pi$ -electrons on the bridging O<sub>2</sub> group. However, VB's results were based on a relatively small number of observed reflections and their final *R* index was

\* Contribution No. 3348 from the Gates and Crellin Laboratories of Chemistry.